

Application of the Macrolayer Dryout Model for the Prediction of Pool Boiling CHF at Inclined Plate

Soo Hyung YANG, Soo Hyung KIM, Won Pil BAEK, and Soon Heung CHANG

Department of Nuclear Engineering
Korea Advanced Institute of Science and Technology
373-1 Kusong-dong, Yusong-gu, Taejeon, Korea 305-701

ABSTRACT

Application of the macrolayer dryout model has been performed to predict CHF at inclined plates. For the identification of the detachment frequency of coalesced bubble, experiments have been performed with high-speed motion analyzer and bubble behaviors at inclined plates have been investigated. Based on the observed bubble behaviors, the detachment frequency of the coalesced bubble is measured and linear relations between detachment frequency and heat flux have been developed. In the case of 60° and 90° inclined plate, the detachment frequency decreases with the increase of heat flux. However, opposite trend has been identified in 30° inclined plate: the detachment frequency increases with the increase of heat flux. Using the correlation of macrolayer thickness suggested by Haramura & Katto and the extrapolation of the identified linear relations, CHF values at different conditions have been predicted. According to the prediction results, CHF values are well predictable.

1. INTRODUCTION

Zuber *et al.* [1] and Kutateladze [2] were the first to provide a theoretical formulation for pool boiling CHF based on the hydrodynamic instability model. Through several decades, the hydrodynamic instability model has been mainly revised by Lienhard *et al.* [3, 4] and suggested one of the most promising models for the prediction of pool boiling CHF at well-wetted large horizontally facing upward plates. However, this model has some drawbacks: difficulty in the consideration of the effect of the heated surface's condition, for example, the wettability, contamination, heat capacity, etc. In addition, several experiments show that whereas some dry areas disappear some time after their creation, others grow and thereby induce burnout of heated surface [5, 6]. These phenomena are difficult to be described with the hydrodynamic instability model. In the application of the hydrodynamic instability model to the situations different from the horizontally facing upward plate, the instability model also has some difficulties for the prediction of the pool boiling CHF. To overcome the limitations of the hydrodynamic instability model and realistically describe phenomenological information related to the bubble behavior at high heat flux and liquid layer existed at the heated surface even at CHF, some kinds of mechanistic models have been suggested. Particularly, the macrolayer dryout model suggested by Haramura & Katto [7] has been widely recognized as alternative of the mechanistic-

tic CHF model and has been applied to different boiling conditions. The macrolayer dryout model is typically represented as following correlation:

$$q_{CHF} = \delta_f \cdot \rho_f \cdot h_{fg} \cdot f \quad (1)$$

Here δ_f and f are macrolayer thickness and detachment frequency of coalesced bubble, respectively.

In this study, the application of the macrolayer dryout model into inclined plates has been performed to predict the pool boiling CHF. In the point of the macrolayer dryout model, the macrolayer thickness and the detachment frequency of the coalesced bubble are very important to predict the pool boiling CHF. For the identification of the detachment frequency of the coalesced bubble, experimental works with high-speed motion analyzer have been performed to investigate the bubble behavior at inclined plate. Based on the recorded bubble behavior, the detachment frequency of the coalesced bubble has been identified. Contrary to the detachment frequency of coalesced bubble, it is difficult to identify the macrolayer thickness with present experimental facility. Therefore detailed analyses have been performed concentrating on experimental works related to macrolayer thickness.

2. BUBBLE BEHAVIOR

Investigation on the bubble behavior at heated surface is important to identify the heat transfer and CHF mechanism, and to develop a mechanistic modeling. In this regard, several experiments have been performed to get insights and information: however, most of them are limited to small heated surface and horizontally facing upward plate and/or vertical position. In addition, the bubble behavior at an inclined plate is not fully investigated till now. For this reason, experimental works with high-speed motion analyzer have been performed to clarify the bubble behavior at an inclined plate. In the experiment, heat flux is increased up to 70% ~ 80% of measured CHF for the protection of test section.

2.1 Boiling Phenomena at Inclined Plates

- Horizontal downward facing surface (0°): At low heat fluxes, small bubbles are generated and stay at a limited number of nucleation sites. The small bubble grows with time and, if larger than the width of heated surface, intermittently escape through lateral side of heated surface. Most of heated surface seems to be wetted with surround fluid. With the increase in the heat flux, bubbles more rapidly grow longitudinal and coalesce with surrounding bubbles to become larger oblate ones, as shown in Fig. 1. When the diameter of a bubble grows to larger than the surface width, it escapes from the heated surface mainly through lateral sides. At this heat flux level, the heated surface is almost wetted with bubble, except for the escape of large coalesced bubble for very short time. At high heat fluxes, bubbles are vigorously generated over the heated surface and large bubbles escape through all sides. In addition, compared to intermediate heat flux, the bubble layer thickness at the heated surface seems to be increased with heat flux. The CHF occurs at an arbitrary point.

- 30° inclined downward surface (Fig. 2): At low heat flux, most of the generated bubble at the heated surface moves to and escape through the upper edge of heated surface with coalesced bubble shape. Sliding up through the heated surface, bubble escape is occasionally happened due to not the bubble size larger than the width of heated surface, but the buoyancy acted on the bubble's intrusion part. As heat flux increases further, the coalescence of bubbles moving upward becomes significant and large bubbles escape mainly through the top edge. A cyclic phenomenon is observed (Fig. 6): (i) formation of a large coalesced bubble in the lower part of the heated surface, (ii) rise of the large bubble along the surface, and (iii) the escape of the large bubble through the top edge and initiation of another large coalesced bubble and (iv) new formation of a large coalesced bubble in the lower part of the heated surface. At high heat fluxes, large bubbles escape through all sides but significant bubble sliding seemed to be occurred. In addition, the bubble layer thickness increases with heat flux, similar to 0°. The CHF generally occurs on the lower part of the heated surface.
- 60° inclined downward surface: Bubbles generated at nucleation site moves to upper edge of the plate and escape with coalesced bubble. Contrary to 30°, the bubbles can only escape through the upper edge. As heat flux further increases, the bubble coalescence is more easily identified and cyclic behavior can be detected. At high heat flux, the bubbles intrude the lateral side of the plate, however, most of bubble escape is established at the upper edge, due to the sweeping flow induced by the coalesced bubble generated at the lower part of heated surface. In addition, the size of coalesced bubble is considerably larger than that of 30°. The snapshots for 60° inclined downward surface are shown in Fig. 3.
- Vertical surface (90°; Fig. 4): At very low heat fluxes, the bubbles generated at the nucleation site move upward along the heated surface without any significant coalescence. As heat flux increases, the bubble coalescence can be initiated at near the bottom position of the plate and large bubbles escape mainly through the top edge. A cyclic phenomenon is also observed: new large coalesced bubble is generated at the bottom position as the coalesced bubble escape through the upper edge. At high heat flux, the size of coalesced bubble is somewhat larger than the width of heated plate, however, most of bubble only escape the upper edge, similar to phenomena of 60°. In addition, small bubble is always generated at the lowermost side of the heated surface and is continuously provided to upper coalesced bubble.
- Horizontal upward surface (180°): The bubbles are generated at limited sites and move upward without any coalescence (isolated bubble region) at low heat flux. These nucleation sites seems to be increased with heat flux. At high heat flux, heated surface is nearly covered with coalesced bubble. In addition, the coalesced bubble detaches from the surface with certain distance, which is somewhat small but similar to the Taylor instability wavelength. The photographs are shown in Fig. 5.

2.2 Detachment Frequency of Coalesced Bubble

As referred in 2.1, a cyclic phenomenon is observed in the inclined plates from medium heat flux region ($\sim 400 \text{ kW/m}^2$) (Fig. 6). As shown in Fig. 6, the bubble behavior of (a) seems to be very similar to that of (f). The coalesced time between two successive coalesced bubbles (Fig. 6 (a) and (f)) is defined as the hovering time of coalesced bubble in present study. With this criterion and recorded films on the bubble behavior, the hovering times of coalesced bubble have been measured for 30° , 60° and 90° inclination angles of each test section. The detachment frequency of coalesced bubble can be calculated to the reciprocal of the hovering time of the bubble. With experimentally measured hovering times, linear functions of the detachment frequency with heat flux have been identified for three different inclination angles of each test section. The linear relations are summarized in Table 1 and the linear relations of W3L10 case are shown in Fig. 7.

Effect of Inclination Angle on Detachment Frequency

At the horizontally facing upward plate, the detachment frequency of the bubble becomes to decrease with the increase of heat flux. In the present experiments, this behavior is also identified in the case of 60° and 90° inclined plate, except for the 60° inclined plate of W4L20. However, somewhat different trend on the detachment frequency has been identified in the 30° inclined plate of all test sections and 60° inclined plate of W4L20: the detachment frequency increases with the increase of heat flux. For the confirmation of experimental results at 30° inclined plate, more experiments have been performed to higher heat flux region and experimental results are provided in Fig. 7 (W3L10 case) and Fig. 8 (W3L20 & W4L20 cases), respectively. As shown in Fig. 7 and Fig. 8, although there is some scattering in the detachment frequency with heat flux, similar behaviors have been identified: the frequency increases with the increase of heat flux.

Size Effect on Detachment Frequency

Figure 9 shows the width effects on the detachment frequency of coalesced bubble. In the case of 60° inclined plate of L10 series, the width effect seems to be somewhat negligible. This is resulted from the comparatively short heated surface: the bubbles easily escape from the heated surface without any influences of width. Similar to 60° inclined plate of L10 series, it is difficult to identify the width effect in 30° inclined plate of L15 series. In the other hand, the width effect on the detachment frequency becomes noticeable with the increase of inclination angle. As shown in Fig. 9 (b), the width effects are clearly shown in 60° and 90° inclined plates: the detachment frequency generally decreases with the increase of the width of heated surface. In the case of L20 series, the width of heated surface affects the detachment frequency of coalesced bubble regardless of inclination angle, as shown in Fig. 9 (c).

Comparison of Previous Experiments

Related to the detachment frequency of coalesced bubble at the horizontally facing upward plate, Davidson & Schueler [8] and Walters & Davidson [9] have suggested a theory that upward motion of a growing bubble is determined by a balance between the buoyancy and inertia of the liquid accom-

panying the growing bubble. Haramura & Katto [7] later used this theory for the prediction of CHF in different boiling situations including pool boiling. The correlation of the hovering time used in Haramura & Katto's model, which is the inverse of the detachment frequency, is as follows:

$$\tau_d = \left(\frac{3}{4\pi} \right)^{1/5} \left[\frac{4(\xi\rho_f + \rho_g)}{g(\rho_f - \rho_g)} \right]^{3/5} v_1^{1/5}, \quad \text{here} \quad \xi = \frac{11}{16} \quad (2)$$

Using the hovering time predicted by equation (2), the detachment frequencies with heat flux are calculated and the results are shown in Fig. 10. For the comparison of present experiment, linear relations of detachment frequency identified in the present investigation also provided in the figure. According to the Davidson and Schueler's theory, the detachment frequency of coalesced bubble decreases with the increase of heat flux. This behavior is observed in 60° and 90° inclined plate. Specially, at high heat flux at 60° inclined plate of W3L10 and W3L15, the behavior of detachment frequency as well as the frequency itself are very similar to those predicted by eq. (2). In the other hand, different trend in the behavior of detachment frequency has been identified in 30° inclined plate.

For the measurement of CHF and detachment frequency with inclination angle, Sakashita *et al.* [10] performed experiment with 15-mm diameter copper disk. According to their experiment, the detachment frequencies at CHF of 30° and 90° inclined plate are about 9.14 and 14.68, respectively. Figure 11 shows Sakashita *et al.*'s and present experimental results. As shown in Fig. 11, there exists considerable difference on the detachment frequencies between two experiments. The difference in the detachment frequency may be induced by the difference in heater size and geometry in each experiment.

3. MACROLAYER THICKNESS

Several experiments have been performed to investigate the behavior of the macrolayer thickness with heat flux at horizontally facing upward plate. Their details and the predictions by developed correlations for the macrolayer thickness are shown in Table 2 and Fig. 12, respectively. As shown in Fig. 12, macrolayer thickness is generally correlated with the inverse proportion of heat flux; however, there are considerable differences between the predictions of those correlations. This is induced by the characteristics of heated surface including surface roughness, wettability, dimensions, and different measuring technique for the macrolayer thickness, i.e., electric resistance probe device, conductivity probe device, photographic study, and so on. In the other hand, Sakashita *et al.* [10] performed experiments to investigate the CHF and detachment frequency of coalesced bubble at downward facing plate, i.e., from 0° to 90°, in water and ethanol pool with 15 mm diameter copper disk. Based on the macrolayer dryout model and the measurements of CHF and the detachment frequency, they calculated macrolayer thickness with the inclination angle of heated surface (Fig. 13). According to their experimental results, macrolayer thickness seems to be somewhat affected by the inclination angle of heated surface. However, Sakashita *et al.* have insisted that the macrolayer thickness at inclined plate can be predictable with correlation suggested by them, which is developed with the experimental data of the macrolayer thickness measured at horizontally facing upward plate and vertical position.

4. ASSESSMENT OF MACROLAYER DRYOUT MODEL

In the viewpoint of macrolayer dryout model, CHF is occurred when the macrolayer dries out prior to the detachment of coalesced bubble. In present work, following criterion is used:

$$\frac{q}{\rho_f \cdot h_{fg} \cdot f(q)} > \delta_f(q) \quad (3)$$

The underlying mechanism is that the CHF occurs when the liquid consumption before bubble departure is larger than the macrolayer thickness at certain heat flux. Related to the macrolayer thickness, the analytical or empirical correlation considering the inclination angle of heated surface is not suggested till now. Therefore it is difficult to find the suitable correlation. The only clue for the selection of macrolayer thickness may be Sakashita *et al.*'s experimental results: i.e. the correlation of macrolayer thickness based on the experimental data at the horizontal facing upward and vertical position is well predictable the macrolayer thickness at the inclined plate. Because of above reason and no experimental coefficient, Haramura & Katto model is arbitrarily selected for the prediction of the macrolayer thickness with heat flux.

Using the Haramura & Katto model as the macrolayer thickness and the extrapolation of the linear fitting relations of the detachment frequency based on the present experimental results, CHF values at different conditions have been predicted as shown in Table 3 and Fig. 14. According to the prediction results, in 30° inclined plate and 60° & 90° inclined plate, CHF values are generally over-predicted and under-predicted, respectively. However, considering the prediction errors, the application of the macrolayer dryout model to the pool boiling CHF seems to be reasonable approach.

5. CONCLUSIONS

Application of the macrolayer dryout model into inclined plates has been performed to predict the pool boiling CHF. In addition, an experimental works have been performed to investigate the bubble behavior at inclined plate and measure the detachment frequency of coalesced bubble. Through analytical and experimental works, important findings are summarized as follows:

1. Above about 400 kW/m², cyclic behaviors have been clearly observed in 30°, 60° and 90° inclined plate: (i) formation of a large coalesced bubble in the lower part of heated surface, (ii) rise of the large bubble along the surface, (iii) the escape of the large bubble through the top edge and initiation of the coalesced bubble's generation at lower position of heated surface, and (iv) new formation of a large coalesced bubble in the lower part of heated surface.
2. Considering the coalesced time between two successive bubbles as the hovering time of coalesced bubble, the detachment frequency of coalesced bubble at an inclined plate has been identified and linear fitting relationships have been developed based on the experimental results. In the case of 60° and 90° inclined plate, the frequency decreases with the increase of heat flux. However,

somewhat different tendency has been identified in 30° inclined plate: detachment frequency increase with the increase of heat flux.

3. With the macrolayer thickness suggested by Haramura & Katto and the extrapolation of linear fitting correlations for bubble detachment frequency, macrolayer dryout model is applied to predict CHF at inclined plate. According to the prediction results, CHF can be well predicted for different conditions. In this point of view, the macrolayer dryout model is thought to be promising approach for the pool boiling CHF.

Nomenclature

| | |
|------------|--|
| f | detachment frequency of coalesced bubble |
| g | gravitational acceleration, m/s ² |
| h_{fg} | latent heat of vaporization, J/kg |
| q | heat flux, kW/m ² |
| q_{CHF} | critical heat flux, kW/m ² |
| v_1 | volumetric growth rate of bubbles, m ³ /sec |
| ν_f | dynamic viscosity of liquid, m ² /sec |
| θ | inclination angle (0° for a horizontal downward-facing plate, 90° for a vertical plate, and 180° for a horizontal upward-facing plate) |
| ρ_f | liquid density, kg/m ³ |
| ρ_g | vapor density, kg/m ³ |
| δ_f | macrolayer thickness, m |
| t_d | hovering time of coalesced bubble |

References

1. N. Zuber, Hydrodynamic Aspects of Boiling Heat Transfer, USAEC Rept. AECU-4439, 1959.
2. Hewitt, G.F., *Chapter 6.4 Burnout*, in *Handbook of Multiphase System*, Vol. 1, 6.66-6.141, Hemisphere Publishing Corporation, Washington, D.C., 1982.
3. Lienhard, J.H. and Dhir, V.K., "Hydrodynamic Prediction of Peak Pool Boiling Heat Flux from Finite Bodies", *ASME J. Heat Transfer*, Vol. 95, 152-158, 1973.
4. Lienhard, J.H., Dhir, V.K. and Rihrer, D.M., "Peak Pool Boiling Heat Flux Measurements on Finite Horizontal Flat Plates," *ASME J. Heat Transfer*, Vol. 95, 477-482, 1973.
5. Kirby, D.B. and Westwater, J.W., "Bubble and Vapor Behavior on a Heated Horizontal Plate during Pool Boiling near Burnout," *Chem. Eng. Prog. Symp. Series*, Vol. 61(57), 238-248, 1965.
6. Van Ouwerkerk, H.J., "Burnout in Pool Boiling: The Stability of Boiling Mechanism," *Int. J. Heat Mass Transfer*, Vol. 15, 25-34, 1972.
7. Y. Haramura and Y. Katto, "A new hydrodynamic model of critical heat flux, applicable widely to both pool and forced convective boiling on submerged bodies in saturated liquids," *Int. J. Heat Mass Transfer*, Vol. 26, 389-399, 1983.
8. Davidson, J.F. and Schueler, O.G., "Bubble Formation at an Orifice in an Inviscid Liquid," *Transaction Inst. Chem. Eng.*, Vol. 38, 335-345, 1960.

9. Walters, J.K. and Davidson, J.F., "The Initial Motion of a Gas Bubble formed in an Inviscid Liquid," *J. Fluid Mechanics*, Vol. 17, 321-340, 1963.
10. Sakashita, H., Yasuda, H. and Kumada, T., "Studies on Pool Boiling Heat Transfer (Modification of Correlation of Macrolayer Thickness and Measurements of Macrolayer Thickness at Lower Heat Fluxes)," *Heat Transfer-Japanese Research*, Vol. 25(8), 522-536, 1996.
11. R.F. Gaertner, "Photographic study of nucleate pool boiling on a horizontal surface, *ASME J. of Heat Transfer*," Vol. 85, 17-29, 1965.
12. Iida, Y. and Kobayashi, K. 1970, "An Experimental Investigation on the Mechanism of Pool Boiling Phenomena by a Probe Method," *4th Int. Heat Transfer Conf.*, Paris-Versailles, B.1.3, 1970.
13. A.M. Bhat, J.S. Saini and R. Prakash, "Role of macrolayer evaporation in pool boiling at high heat flux," *Int. J. Heat Mass Transfer*, Vol. 29(12), 1953-1961, 1986.
14. M. Shoji, "A study of steady transition boiling of water: experimental verification of macrolayer evaporation model," *Proc. the Eng. Found. Conf. On Pool and External Flow Boiling*, Santa Barbara California, 237-242, 1992.
15. Rajvanshi, A.K., Saini, J.S. and Prakash, R., "Investigation of Macrolayer Thickness in Nucleate Pool Boiling at High Heat Flux," *Int. J. Heat and Mass Transfer*, Vol. 35(2), 343-350, 1992.
16. Kumada, T., Sakashita, H. and Yamagishi, H., "Pool Boiling Heat Transfer-II. Thickness of Liquid Macrolayer formed beneath Vapor Masses," *Int. J. Heat and Mass Transfer*, Vol. 38(6), 979-987, 1995.

Table 1. Bubble Detachment Frequency

| T/S | 30° | 60° | 90° |
|-------|--------------------------------|----------------------------------|----------------------------------|
| W3L10 | $F = 12.35 + 0.00171 \times q$ | $F = 13.42 - 0.00101 \times q$ | $F = 13.51 - 0.000622 \times q$ |
| W3L15 | $F = 11.35 + 0.00295 \times q$ | $F = 13.57 - 0.001 \times q$ | $F = 15.96 - 0.004 \times q$ |
| W3L20 | $F = 11.94 + 0.00372 \times q$ | $F = 13.55 - 0.000509 \times q$ | $F = 13.81 - 0.00115 \times q$ |
| W4L10 | - | $F = 12.57 - 0.0002378 \times q$ | - |
| W4L15 | $F = 10.01 + 0.00456 \times q$ | $F = 12.91 - 0.00175 \times q$ | $F = 12.44 - 0.0008814 \times q$ |
| W4L20 | $F = 9.37 + 0.00405 \times q$ | $F = 10.85 + 0.00111 \times q$ | $F = 13.48 - 0.00248 \times q$ |

Table 2. Detailed Information related to the Experiment for the Macrolayer Thickness

| Author | Dia. of Test Section | Measurement Device | Correlation of the Macrolayer Thickness |
|------------------------------|---------------------------------|-----------------------------|--|
| Gaertner [11] | 50.48 mm | Photographic study | $\delta_f = 0.4854 \times 10^5 q^{-1.4225}$ |
| Iida & Kobayasi [12] | 20 mm | Conductivity probe | $\delta_f = 3.2296 \times 10^5 q^{-1.5148}$ |
| Bhat <i>et al.</i> [13] | 42 mm | Conductivity probe | $\delta_f = 1.585 \times 10^5 q^{-1.527}$ |
| Shoji [14] | 10 mm | Electric impedance method | $\delta_f = 1.77 \times 10^4 q^{-1.38}$ |
| Rajvanshi <i>et al.</i> [15] | 50 mm | Electrical resistance probe | $\delta_f = 0.0107 \rho_g \sigma (\rho_g / \rho_f)^{0.4} (h_{fg} / q)$ |
| Kumada <i>et al.</i> [16] | 2~30 mm disks 0.2~3 mm wires | Conductance probe | $\delta_f = 0.786 [v_f^8 \sigma^{11} / \{\rho_f^6 g^5 (\rho_f - \rho_g)^5\}]^{1/24} / G_0^{5/6}$ |

Table 3. Prediction Results based on Macrolayer Dryout Model

| | 30° | | 60° | | 90° | |
|-------|------|---------------|------|--------------|------|---------------|
| | M. | P. (Err) | M. | P. (Err) | M. | P. (Err) |
| W3L10 | 1156 | 1170 (+1.2%) | 1129 | 1110 (-1.7%) | 1196 | 1130 (-5.5%) |
| W3L15 | 1186 | 1190 (+0.3%) | 1189 | 1120 (-5.8%) | 1275 | 1090 (-14.5%) |
| W3L20 | 1215 | 1230 (+1.2%) | 1145 | 1130 (-1.3%) | 1196 | 1120 (-6.4%) |
| W4L10 | 1241 | | 1166 | 1110 (-4.8%) | 1210 | |
| W4L15 | 1088 | 1200 (+10.3%) | 1109 | 1070 (-3.5%) | 1159 | 1090 (-6.0%) |
| W4L20 | 1097 | 1097 (+5.7%) | 1098 | 1110 (+1.1%) | 1120 | 1070 (-4.5%) |

*Err. = (P-M)/P



Fig. 1 Bubble Behavior at 0° Inclined Plate of W4L20 (50, 200 and 500 kW/m²)



Fig. 2 Bubble Behavior at 30° Inclined Plate of W3L10 (98, 492 and 800 kW/m²)



Fig. 3 Bubble Behavior at 60° Inclined Plate of W3L10 (104, 402 and 852 kW/m²)

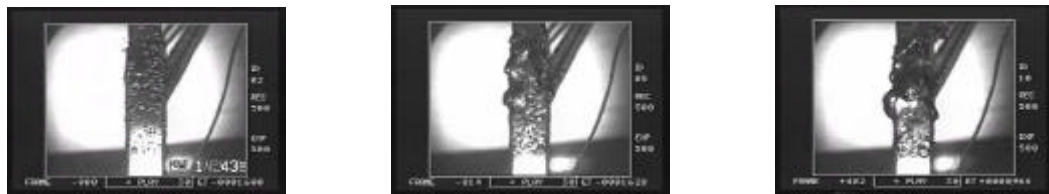


Fig. 4 Bubble Behavior at 90° Inclined Plate of W3L10 (99, 402 and 800 kW/m²)



Fig. 5 Bubble Behavior at 180° Inclined Plate of W3L10 (91, 600 and 799 kW/m²)

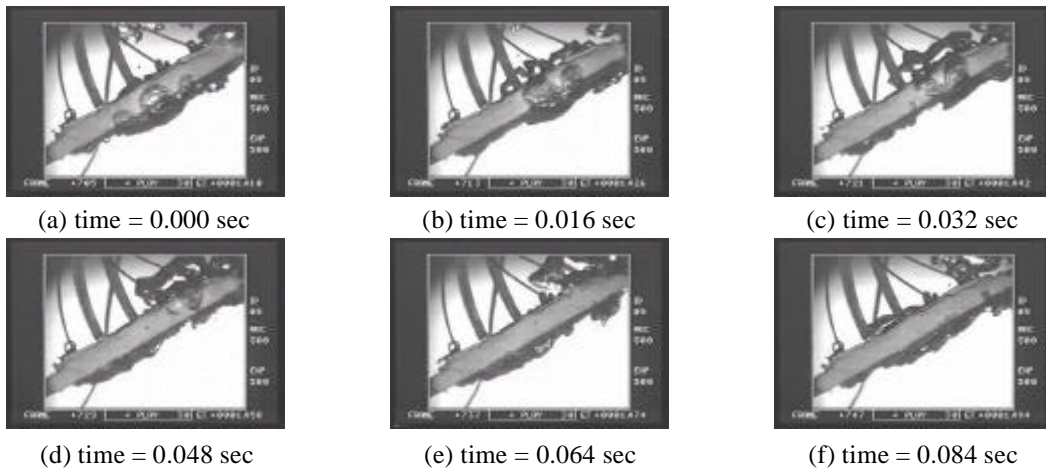


Fig. 6 Cyclic Behavior (W3L10 and 30°; 492 kW/m²)

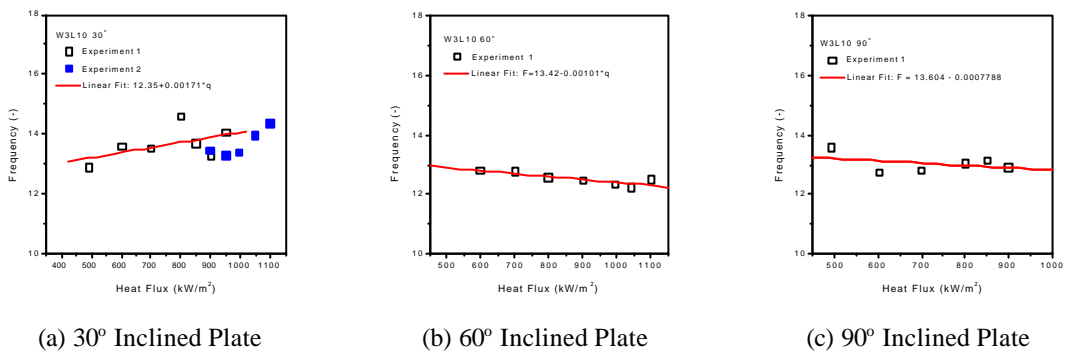


Fig. 7 The Detachment Frequency of Coalesced Bubble at W3L10

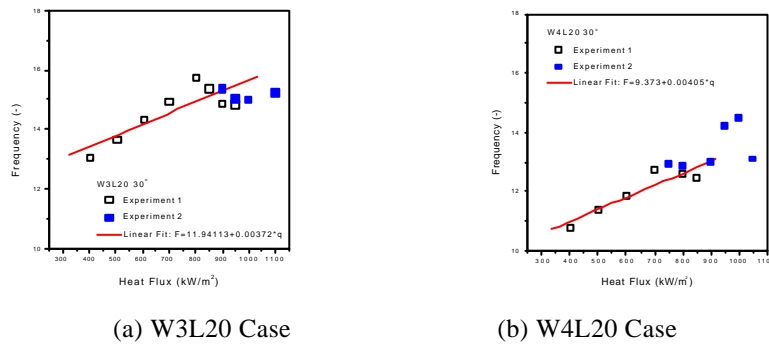
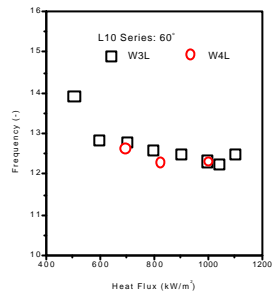
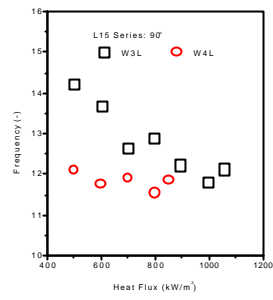
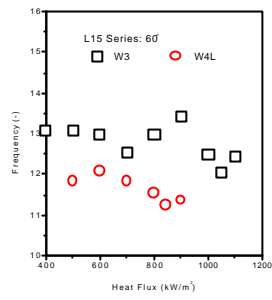
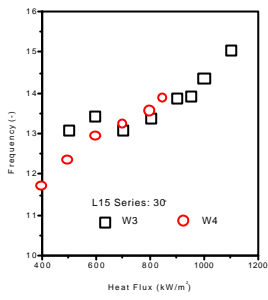


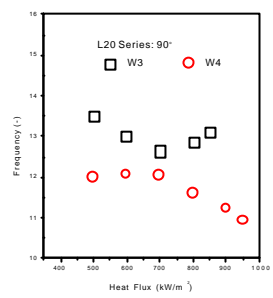
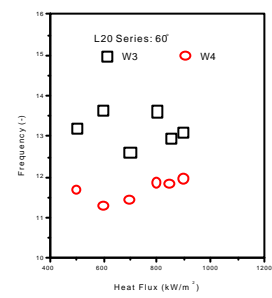
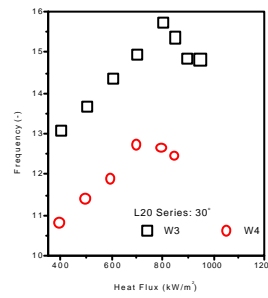
Fig. 8 The Detachment Frequency at High Heat Flux Region



(a) L10 Series
(b)

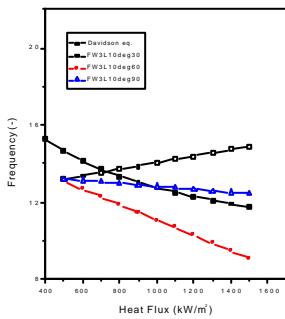


(b) L15 Series

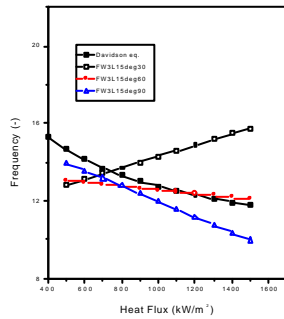


(c) L20 Series

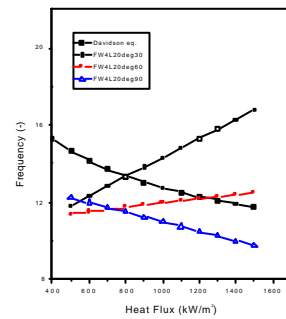
Fig. 9 The Effect of Heater Width on the Detachment Frequency



(a) W3L10 Case



(b) W3L15 Case



(c) W4L20 Case

Fig. 10 Comparison of the Prediction and Davidson *et al.*'s Theory

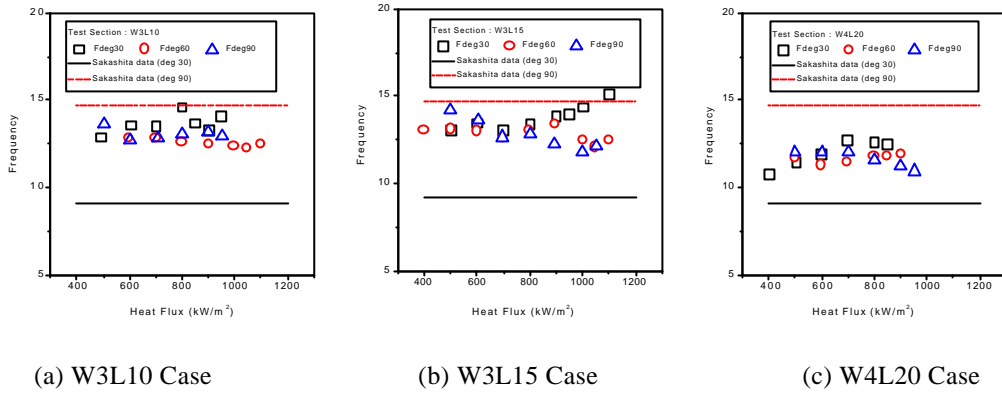


Fig. 11 Comparison of Present and Sakashita *et al.*'s Experiment

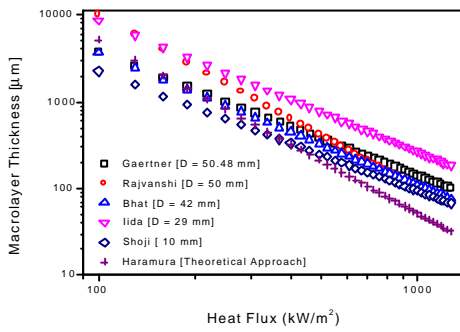


Fig. 12 Behavior of Macrolayer Thickness with Heat Flux

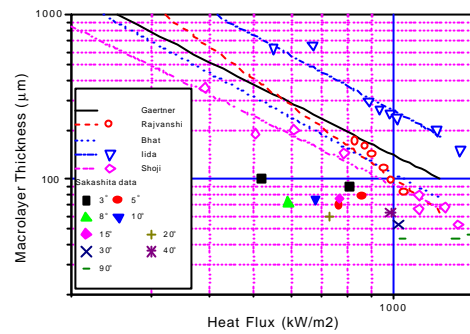
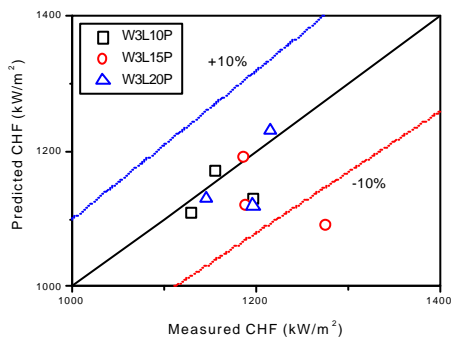
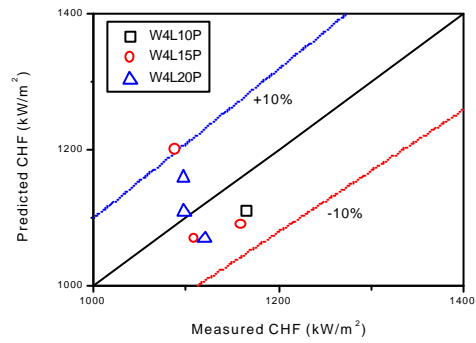


Fig. 13 Comparison of Kumada & Sakashita's Experiment and Other's Works



(a) W3 Series



(b) W4 Series

Fig. 14 CHF Prediction Results